Lyot depolarizer in terms of the theory of coherence—description for light of any spectrum

Piotr L. Makowski,[1,*] Marek Z. Szymanski,[1,2] and Andrzej W. Domanski[1]

[1]Faculty of Physics, Warsaw University of Technology, Koszykowa 75, 00-662 Warsaw, Poland

[2]Commissariat à l'énergie atomique et aux énergies alternatives Grenoble, Institut Nanosciences et Cryogénie/Structure et Propriétés d'Architectures Moleculaires/Laboratoire d'Electronique Moléculaire Organique & Hybride, 17 rue des Martyrs, 38054 Grenoble cedex 9, France

*Corresponding author: makowski@if.pw.edu.pl

Received 27 September 2011; accepted 30 November 2011;
posted 13 December 2011 (Doc. ID 154437); published 8 February 2012

A coherence-based description of the Lyot depolarizer illuminated by polychromatic light of any spectral density distribution is proposed as a generalization of the formulas provided for symmetrical spectra by Burns [J. Lightwave Technol. **1**, 475 (1983)] and Mochizuki [Appl. Opt. **23**, 3284 (1984)]. The structure of the derived expressions is explained in physical terms, and a numerical comparison with the previous solutions is performed. The results of the numerical analysis show that the proposed description, when applied to any configuration of a two-segment anisotropic depolarizer, is fully equivalent with the Mueller–Stokes calculus for broadband light. Following this consistency, the range of accuracy of the formula by Mochizuki has been verified.

OCIS codes: 030.0030, 260.5430, 200.4860.

1. Introduction

Polarization properties of light significantly affect performance of photonic systems because most of the basic optical phenomena like transmission, reflection, interference, gain and detection of optical radiation are polarization dependent [1]. In order to immunize the intrinsic states of polarization from unwanted external conditions, designers often make use of unpolarized light, i.e., light with significantly decreased degree of polarization (DoP). Three kinds of depolarization are distinguished in terms of the domain of polarization states' scrambling: (a) spatial (e.g., wedge depolarizers in free space), (b) temporal (rotating-retarder scramblers, recently developed fiber-optic ring depolarizers [2,3]), and (c) spectral (the Lyot depolarizer principle). The last type, which is the subject of this paper, is the most commonly used due to the simple, passive configuration and its applicability in all-fiber systems.

Although the Lyot depolarizer has been known since 1929 [4], the first successful attempt to its quantitative description did not appear until Billings [5] carried the optimization problem of a two-segment static crystal depolarizer in terms of statistical optics. His work, concerning a rectangular-shaped spectrum only, has been extended for the case of blackbody radiation by Loeber [6]. From that point, the original configuration of the Lyot depolarizer was theoretically justified. Later works by Burns [7] and Mochizuki [8] took an issue of an alternative description utilizing the contemporary achievements of the theory of coherence, leading to direct depolarization formulas for light of any spectrum symmetrical with respect to the central wavelength. Since then, great progress has been done in the field [9–11]; nevertheless, no attempts to simplify or generalize the reasoning in [7,8] seem to be taken to this day. The aim of this work is to provide an improved version of the description [8], suitable for light of any spectral density profile.

1559-128X/12/050626-09$15.00/0

2. Coherency Matrix without the Quasi-Monochromatic Regime

We consider a continuous lightwave of an arbitrary spectral density distribution emerging from a secondary source whose angular size at the input plane of the optical system is negligible. We also assume that the radiation enters the optical system as a collimated beam. In practice these conditions are well suited for all kinds of LEDs as well as fiber-optic sources equipped with a collimating lens. In the case of gas-discharge lamps or incandescent sources, the light has to pass through a pinhole or other small aperture to obey these conditions (Fig. 1).

The restrictions applied above drive to a model of a uniform and fully spatially coherent collimated light beam that can be completely described by a vector: $\mathbf{U}(z,t) = [U_x(z,t), U_y(z,t)]$, where the Cartesian components of the electric or magnetic field, $U_x(z,t)$ and $U_y(z,t)$, are considered as real-valued realizations of two stochastic processes, stationary at least in the wide sense [9–11]. Within the framework of the generalized function theory, it is convenient to represent the electric field by a vector of complex analytic signals: $\mathbf{E}(z,t) = [E_x(z,t), E_y(z,t)]$.

It is a common knowledge [9] that, in the quasi-monochromatic approximation, polarization properties of a uniform well-collimated beam can be described in the space–time domain by the four elements of the Hermitian and nonnegative definite coherency matrix (or polarization matrix) and that the DoP of such beam can be expressed by the trace and determinant of the coherency matrix:

$$\mathbf{J}_{ij} = \langle E_i^{(\mathrm{qm})*}(z,t) E_j^{(\mathrm{qm})}(z,t)\rangle, \tag{1a}$$

$$\mathrm{DoP} = \sqrt{1 - (4\,\mathrm{Det}\,\mathbf{J})/(\mathrm{Tr}\,\mathbf{J})^2}, \tag{1b}$$

where $i = x,\ y$, $j = x,\ y$, and $E_i^{(\mathrm{qm})}(z,t)$ is the complex analytic signal associated with the quasi-monochromatic electric field waveform, hence superscript (qm). The $*$ denotes complex conjugate, and the sharp brackets denote averaging over the statistical ensemble of the possible realizations of this waveform with respect to their occurrence probability. In the case of a physical source with a sufficiently stable spectrum, the ensemble average can be replaced by the time average over a finite time period.

At this point one can ask: how does the quasi-monochromatic approximation affect Eqs. (1)? The reasoning conducted in [9] (Subsection 6.3.3) that leads to Eq. (1b) is based on three properties of the coherency matrix Eq. (1a):

(i) $\mathbf{J}$ is Hermitian.
(ii) $\mathbf{J}$ is nonnegative definite.
(iii) Due to the incoherent summation of independent fields, $\mathbf{J}$ can be expressed as a sum of matrices of the fully polarized and unpolarized portion of the light beam.

It appears that none of these conditions depends on the bandwidth of the light in fact. Although the called derivation is performed on the matrix $\mathbf{J}$ defined only for quasi-monochromatic waves $E_i^{(\mathrm{qm})}(z,t)$, this particular property of $E_i(z,t)$ is never used, neither directly nor indirectly, while arriving to Eq. (1b). Therefore, it is reasonable to define generalized forms of the coherence matrix Eq. (1a) and DoP Eq. (1b) concerning any stationary stochastic process:

$$\Gamma_{ij} = \langle E_i^*(z,t) E_j(z,t)\rangle, \tag{2a}$$

$$\begin{aligned}\mathrm{DoP} &= \sqrt{1 - (4\,\mathrm{Det}\,\Gamma)/(\mathrm{Tr}\,\Gamma)^2} \\ &= \sqrt{1 - 4(\Gamma_{xx}\Gamma_{yy} - |\Gamma_{xy}|^2)/(\Gamma_{xx} + \Gamma_{yy})^2},\end{aligned} \tag{2b}$$

where $E_i(z,t)$ refers to a Cartesian component of the collimated uniform beam of any spectral density shape (Fig. 1). It should be pointed out that Eqs. (2) are not expected to obey any relations with quantities measured by use of a linear retarder. That is because, in the case of broadband light, any time delay introduced by a retarder must be considered as comparable to the coherence time of the radiation. Thus, the classical methods [1] cannot be employed directly in precise measurements of DoP expressed by Eq. (2b). One possible solution is to use a Fresnel rhomb providing achromatic quarter-wave retardation. Another one involves spectroscopic polarimetry [12]. In any case, the spectral representation of a stochastic process has to be used [9,11].

However, Eqs. (2) are consistent with definitions of the complex mutual coherence function (complex cross correlation) and the complex degree of coherence [9],

$$\Gamma_{12}(\tau) = \langle E_1^*(t) E_2(t+\tau)\rangle, \qquad \Gamma_{21}(\tau) = \Gamma_{12}^*(-\tau), \tag{3}$$

$$\gamma_{12}(\tau) = \frac{\Gamma_{12}(\tau)}{\sqrt{\Gamma_{11}(0)\Gamma_{22}(0)}}, \qquad \gamma_{21}(\tau) = \gamma_{12}^*(-\tau), \tag{4}$$

as well as with the Wiener–Khintchine theorem,

$$\Gamma_{11}(\tau) = \int_{-\infty}^{+\infty} G(\omega) e^{-i\omega\tau}\,\mathrm{d}\omega, \tag{5}$$

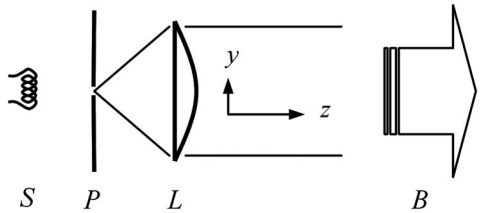

Fig. 1. Model of a collimated polychromatic beam: S, arbitrary light source; P, pinhole; L, collimating lens; B, uniform and fully spatially coherent beam with negligible divergence.

where $G(\omega)$ denotes the spectral density distribution of the stochastic process associated with an arbitrary Cartesian component in the cross section of the beam (Fig. 1) and $\Gamma_{11}(\tau)$ is the complex autocorrelation function of that process. Note that the elements of the generalized coherency matrix Eq. (2a) are exactly the complex mutual coherence functions with $\tau = 0$. Equations (3)–(5) are general enough only in the considered case of one-dimensional propagation and full spatial coherence.

3. Mueller–Stokes Calculus for a Collimated Polychromatic Beam

The Mueller–Stokes (M–S) matrix formalism is a convenient method for handling cascade linear transformations of partially polarized light. Although in popular textbooks like [1] this method is introduced for quasi-monochromatic plane waves only, it is also capable of computing state of polarization (SoP) and DoP for any spectral composition of plane waves, as has been exploited by Billings [5] and Loeber [6] in their papers concerning the Lyot depolarizer. A similar approach for broadband light based on spectral coherency matrices and the Jones calculus can be found in later works [13].

The M–S method for arbitrary spectra has been reviewed in detail in [14]. The second-order statistical properties of a partially polarized beam are represented by the real-valued Stokes vector, which can be expressed by the elements of the coherence matrix Eq. (2a):

$$\begin{aligned}\mathbf{S} &= [S_0, S_1, S_2, S_3]^T \\ &= [\Gamma_{xx} + \Gamma_{yy}, \Gamma_{xx} - \Gamma_{yy}, \Gamma_{xy} + \Gamma_{yx}, i(\Gamma_{yx} - \Gamma_{xy})]^T \\ &= [\Gamma_{xx} + \Gamma_{yy}, \Gamma_{xx} - \Gamma_{yy}, 2\,\mathrm{Re}\{\Gamma_{xy}\}, 2\,\mathrm{Im}\{\Gamma_{xy}\}]^T, \quad (6)\end{aligned}$$

where i indicates the imaginary unit, $\mathrm{Re}\{\bullet\}$ and $\mathrm{Im}\{\bullet\}$ returns the real part and the imaginary part of a complex number, respectively, and the superscript T indicates the vector transposition. The last equality in Eq. (6) comes from hermiticity of the matrix Eq. (2a). For the reasons discussed in Section 2, we invoke elements of the coherence matrix of the generalized meaning [Eq. (2a)] instead of the quasi-monochromatic one [Eq. (1a)]. The Stokes vector is transformed by multiplication by the 4×4 real-valued Mueller matrix describing the cascade of linear optical elements or other linear operations. In the case of polychromatic radiation, the resulting Stokes vector is obtained by incoherent summation of vectors describing individual spectral components at the output plane. If we assume that the input wave is fully polarized (DoP = 1), which also implies that all spectral components possess the same SoP and DoP = 1, then we have

$$\mathbf{s}^{\mathrm{out}} = \left(\int_0^{+\infty} \mathbf{M}(\omega) \hat{G}(\omega) \mathrm{d}\omega \right) \cdot \mathbf{s}^{\mathrm{in}}, \quad (7)$$

where $\mathbf{s}^{\mathrm{in}}$ and $\mathbf{s}^{\mathrm{out}}$ are the normalized (such that $s_0 = 1$) Stokes vectors at the input and output plane of the system, respectively, $\mathbf{M}(\omega)$ is the spectral Mueller matrix of the system (dependency on ω introduces the phase dispersion) and $\hat{G}(\omega)$ is the normalized power spectral density distribution. The residual DoP of the beam $\mathbf{s}^{\mathrm{out}}$ is then obtained by

$$\mathrm{DoP} = \frac{\sqrt{s_1^2 + s_2^2 + s_3^2}}{s_0}. \quad (8)$$

Substituting the definition Eq. (6) to Eq. (8) shows that Eq. (8) is equivalent to Eq. (2b).

It is worth noticing that the M–S calculus, unlike the depolarization formulas from [7,8], operates directly on the spectral components and involves real quantities only. This difference in the reasoning makes the M–S method an interesting reference in study on complex coherence-based approaches.

4. Proposal of a Coherence-Based Description

We consider a static depolarizer originating from the classic Lyot configuration [4]. In the bulk version, it consists of two anisotropic uniaxial crystals cut with respect to their birefringence axes oriented perpendicularly to the propagation direction. We assume that both segments are made of the same material described along the z axis by the linear birefringence $\Delta n = n_y - n_x > 0$, while their lengths L_1,L_2, and the twist angle θ are variable (Fig. 2). We neglect dispersion of Δn as well as transmission and reflection losses. We assume that the device is illuminated with a well-collimated beam of an arbitrary spectrum (Fig. 1). This implies that the coherence area of the beam exceeds the cross-section area of the crystals.

Only the linearly polarized waves at input are examined. There are two reasons for that: (1) the

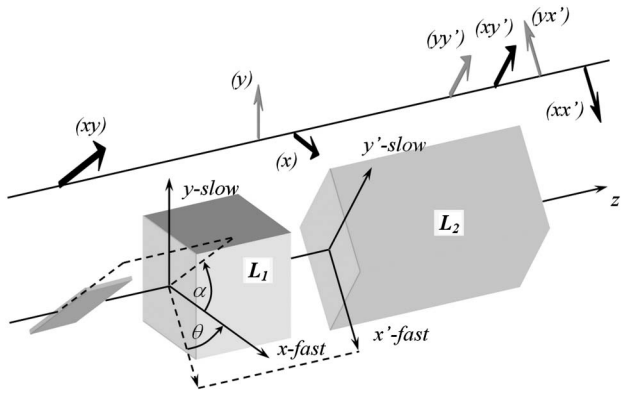

Fig. 2. Two-segment crystal depolarizer with an arbitrary twist angle $\theta > 0$ and variable segment lengths L_1 and L_2; $\alpha > 0$ is the azimuth of the incident linearly polarized wave. The xy and $x'y'$ coordinate systems are matched to the birefringence axes of the crystals. Above, the amplitude decomposition between the fast and slow axes is shown. The segments L_1, L_2 induce time delays τ_1, τ_2 between light components parallel to the axes of the corresponding coordinate systems.

incident radiation (or its portion considered) has to be fully polarized (DoP = 1) to allow unambiguous description of the residual DoP of the system without specifying the history of the beam and (2) variable input azimuth of the linearly polarized monochromatic wave together with variable retardation (induced by L_1) is sufficient to produce an elliptically polarized beam of any orientation and ellipticity at the joint plane [1].

Using the introduced model of the polychromatic beam (Fig. 1) we shall determine the coherency (polarization) matrix Eq. (2a) of light emerging from the system (Fig. 2). Suppose that the analytic signal associated with the incident radiation is $E(t)$, while τ_1 and τ_2 are the time delays induced between the fast and slow axis in the segments L_1 and L_2, respectively. The time delay τ describes completely the influence of a birefringent segment as long as the optical dispersion of the material is negligible. Projecting the initial disturbance $E(t)$ on the birefringence axes and applying proper time delays to the resulting components, we arrive to expressions for the output components in the $x'y'$ coordinate system:

$$\begin{cases} E_{x'} = E(t+\tau_1+\tau_2)\cos(\alpha)\cos(\theta) - E(t+\tau_2)\sin(\alpha)\sin(\theta) \\ E_{y'} = E(t)\sin(\alpha)\cos(\theta) + E(t+\tau_1)\cos(\alpha)\sin(\theta). \end{cases} \tag{9}$$

Now we can build the coherence matrix Eq. (2a) in the coordinate system of the second crystal:

$$\Gamma_{x'x'} = \langle E^*_{x'} E_{x'} \rangle, \qquad \Gamma_{x'y'} = \langle E^*_{x'} E_{y'} \rangle, \Gamma_{y'x'} = \Gamma^*_{x'y'}, \qquad \Gamma_{y'y'} = \langle E^*_{y'} E_{y'} \rangle. \tag{10}$$

After substituting Eq. (9) to Eq. (10), every element of the coherency matrix is a sum of four averages, which all are autocorrelation functions of the initial disturbance $E(t)$ with various delays. Thus, using the definitions of Eqs. (3) and (4), we can replace them with complex mutual coherence functions and then with complex self-coherence functions $\gamma_{11}(\tau)$ with proper arguments. With the help of some trigonometric transformations, the coherence matrix of the polychromatic light emerging from the depolarizer can be finally expressed by

$$\Gamma_{x'x'} = I \times \left[\cos^2(\alpha+\theta) + \sin(2\alpha)\sin(2\theta)\frac{1-\gamma^{(r)}_{11}(\tau_1)}{2} \right], \tag{11a}$$

$$\Gamma_{y'y'} = I \times \left[\sin^2(\alpha+\theta) - \sin(2\alpha)\sin(2\theta)\frac{1-\gamma^{(r)}_{11}(\tau_1)}{2} \right], \tag{11b}$$

$$\Gamma_{x'y'} = \frac{1}{2} I \times \{ \cos(2\alpha)\sin(2\theta)\gamma^*_{11}(\tau_2) + \sin(2\alpha)\cos^2(\theta)\gamma^*_{11}(\tau_1+\tau_2) - \sin(2\alpha)\sin^2(\theta)\gamma^*_{11}(\tau_2-\tau_1) \}, \tag{11c}$$

$$\Gamma_{y'x'} = \Gamma^*_{x'y'}, \tag{11d}$$

where $\gamma^{(r)}_{11}(\tau) = \mathrm{Re}\{\gamma_{11}(\tau)\}$ and $I = \Gamma_{11}(0) = \langle E^*(t)E(t) \rangle$ is proportional to the average length of the Poynting vector in every point in the system. In Eq. (11c) the complex self-coherence is complex conjugated to keep the argument positive (when possible) under convention of making x and x' the fast axes. Equations (11) along with Eq. (2b) give residual DoP of light of any spectral density distribution. We propose this model as a generalization of the widely used one provided by Mochizuki [8] for spectra symmetrical with respect to the central frequency.

Equations (11a–11c) can be given a clear geometrical interpretation. The two real quantities $\Gamma_{x'x'}$ and $\Gamma_{y'y'}$ are proportional to intensities of the two orthogonal linearly polarized components of the optical field. The first terms in Eqs. (11a) and (11b) originate from projections of the signal $E(t)$ on the x' and y' axes, respectively. However, the intensity division between x' and y' axes also depends on the SoP at the joint plane (between the segments), and that SoP is represented by $\gamma^{(r)}_{11}(\tau_1)$. This influence vanishes when (a) $\sin(2\alpha) = 0$ only one axis of the first segment is excited, which implies the initial SoP remaining unchanged during propagation through L_1, (b) $\sin(2\theta) = 0$ the twist angle is 0° or 90°. Equation (11c) is complex valued and represents the cross correlation between the components $E_{x'}$ and $E_{y'}$. The individual terms in Eq. (11c) represent all possible interactions between four components propagating through L_2: (xx'), (xy'), (yx'), (yy') that result from double decomposition of the initial disturbance $E(t)$ denoted symbolically as (xy) (the upper part of Fig. 2). The meanings of the terms in Eq. (11c) are as follows. (a) $\cos(2\alpha)\sin(2\theta)\gamma^*_{11}(\tau_2)$ is the decorrelation between two pairs of components, (xx'),(xy') and (yx'),(xy') induced by τ_2; plays role only when the twist angle θ is close to 45°, provided that one of the axes of L_1 carries most of the total intensity. (b) $\sin(2\alpha)\cos^2(\theta)\gamma^*_{11}(\tau_1+\tau_2)$ is the decorrelation between the pair (xx'), (yy'); most significant when θ is close to 0°, provided that both of the axes of L_1 were excited. (c) $-\sin(2\alpha)\sin^2(\theta)\gamma^*_{11}(\tau_2-\tau_1)$ is responsible for the compensation of depolarization effect; most significant when θ is close to 90°, provided that both of the axes of L_1 were excited.

5. Methodology of Numerical Examination

Equations (11) have been tested numerically along with two other approaches: (a) the formula by Mochizuki [8] for symmetrical light spectra and (b) the M–S calculus for an arbitrary spectrum.

The formula by Mochizuki [8] for DoP of light leaving the two-segment depolarizer can be rewritten in accordance with Fig. 2 as

$$\begin{aligned}\mathrm{DoP} = \{&\cos^2(2\alpha)[\cos^2(2\theta) + \sin^2(2\theta)|\gamma(\tau_2)|^2] \\ &+ \sin^2(2\alpha)[1/2\sin^2(2\theta)|\gamma(\tau_1)|^2 \\ &+ \cos^4(\theta)|\gamma(\tau_1+\tau_2)|^2 + \sin^4(\theta)|\gamma(\tau_2-\tau_1)|^2] \\ &- \sin(4\alpha)\sin(2\theta)|\gamma(\tau_2)| \times [\cos^2(\theta)|\gamma(\tau_1+\tau_2)| \\ &- \sin^2(\theta)|\gamma(\tau_2-\tau_1)|]\cos(\omega_0\tau_1) \\ &+ 1/2\sin^2(2\alpha)\sin^2(2\theta)|[\gamma(\tau_1)|^2 - |\gamma(\tau_2-\tau_1)| \\ &\times |\gamma(\tau_1+\tau_2)|]\cos(2\omega_0\tau_1)\}^{1/2}, \end{aligned} \tag{12}$$

where ω_0 denotes the central angular frequency in the spectral density distribution. The solution in [8] has been introduced for an all-fiber version of the device within the framework of the weak guiding approximation, with no coupling between the polarization modes and with negligible dispersion of the effective birefringence. In this case there is a full analogy between linearly polarized modes in a birefringent single-mode fiber and Cartesian field components in a uniaxial anisotropic crystal [15]. Thus, the conditions restricting the use of Eq. (12) are the same as we provided for (11) plus the requirement of the spectral profile symmetrical with respect to the central frequency ω_0.

The proposed approach combining Eqs. (11) and (2b) should be then considered as a generalization of Eq. (12) for any spectral profile. In the case of the optimal Lyot configuration ($\theta = 45°$), Eq. (12) reduces to the expression obtained by Burns [7].

In the M–S method, the resulting Mueller matrix of the depolarizer is obtained by the product

$$\mathbf{M}(\omega) = \mathbf{M}_2(\omega) \cdot \mathbf{T}(-\theta) \cdot \mathbf{M}_1(\omega), \tag{13}$$

where $\mathbf{M}_1(\omega)$ and $\mathbf{M}_2(\omega)$ are the spectral Mueller matrices of the two quartz wave plates expressed in the corresponding coordinate systems (Fig. 2), while $\mathbf{T}(-\theta)$ is a matrix performing rotation of the temporary coordinate system from xy to $x'y'$. Similar to the proposed method Eqs. (11) and (2b), this model does not impose any restrictions on shape and width of the light spectrum.

In order to compare different computational methods, we should provide exactly the same input data for each of them. The required quantities include parameters of the depolarizer plus the characterization of the passing light, that is,

(i) $\gamma_{11}(\tau)$ for the proposed model Eqs. (11) and (2b).
(ii) $|\gamma_{11}(\tau)|$ and ω_0 for Eq. (12) by Mochizuki [8].
(iii) $G(\omega)$ for the M–S method.

Comparing (i) and (iii) is trivial because, according to the Wiener–Khintchine theorem Eq. (5), the complex coherence function $\gamma_{11}(\tau)$ contains the same information as the power spectral density $G(\omega)$. Unfortunately, it is no longer the case when dealing with (ii), as the choice of ω_0 for given $G(\omega)$ is ambiguous in general. In case of an irregular spectrum, it is necessary to specify some constraints on ω_0 to ensure the best comparison conditions. In the presented analysis, the following procedure for finding ω_0 has been conducted.

(i) First, the initial value ω_{00} is obtained by the commonly used integral [9]:

$$\omega_{00} = \frac{\int_0^{+\infty} \omega G^2(\omega)\mathrm{d}\omega}{\int_0^{+\infty} G^2(\omega)\mathrm{d}\omega}. \tag{14}$$

(ii) We define the phase of the cross correlation of the components E_x and E_y at the joint plane:

$$\phi(\tau_1) = -\arg\{\gamma_{11}(\tau_1)\} = \arg\{\langle E_x^*(L_1,t)E_y(L_1,t)\rangle\}, \tag{15}$$

where $\arg\{\bullet\}$ returns the argument of a complex number in the polar representation. It implies from the proportionality $E(t) \propto \exp(-i\omega t)$, along with the convention "x-fast," that $\phi(\tau_1) > 0$ for $\tau_1 > 0$. The right-hand equality in Eq. (15) results from the geometrical relations $E_x(t) = E(t+\tau_1)\cos(\alpha)$ and $E_y(t) = E(t)\sin(\alpha)$ (Fig. 2) substituted to Eqs. (3) and (4). Note that $\phi \in [0; 2\pi]$, and it does not depend on the azimuth α. In the case of strictly monochromatic light, $\phi(\tau_1)$ is simply the retardation (divided modulo 2π) induced by the segment L_1. In the case of quasi-monochromatic light, it can be interpreted as the retardation for the central frequency ω_0 disturbed by the phase of cross correlation of the envelopes (complex amplitudes) of the x,y components of the field [9]. In the most general case of an arbitrary spectrum, the equality Eq. (15) is still correct, although the interpretation associating $\phi(\tau_1)$ with the retardation for some frequency ω_0 is not meaningful anymore as the concept of the signal envelope cannot be applied.

(iii) Finally, the initial value ω_{00} [Eq. (14)] is slightly scaled to ω_0 so that

$$\phi_{\omega_0}(\tau_1) = \phi(\tau_1), \tag{16}$$

where $\phi_{\omega_0}(\tau_1) = \omega_0\tau_1$ is obtained through Eq. (15) for a strictly monochromatic wave with frequency ω_0. We note that $\phi_{\omega_0} \in [-\infty; \infty]$, while in the case of numerically resolved $\phi(\tau)$ the domain expansion is possible only in specific intervals of τ where $|\gamma_{11}(\tau)| > 0$.

The above procedure assures that the value $\gamma_{11}^{(r)}(\tau_1)/|\gamma_{11}(\tau_1)|$ is set equal for both the polychromatic beam and the component ω_0 required by Eq. (12). This will not make the corresponding normalized Stokes vectors equal for τ_1 (because s_1 is never affected by depolarization in a single crystal, unlike s_2 and s_3), but it provides comparison conditions that account the influence of the internal

SoP on the performance of the depolarizer (also discussed in [14]).

It is convenient to have a precise control on the internal SoP for a given depolarizer and spectrum of light. For this reason we define the retardation change $\Delta\phi$ of the component ω_0 in the following way:

$$\Delta\phi(\tau_1') = \phi_{\omega_0}(\tau_1') - \phi_{\omega_0}(\tau_1^{(0)}), \tag{17a}$$

$$\phi_{\omega_0}(\tau_1^{(0)}) = 2k\pi, \qquad k \in \mathbf{N}, \tag{17b}$$

where τ_1' is a free variable and $\tau_1^{(0)}$ is obtained by the minimal required adjustment of the given system parameter τ_1 that makes Eq. (17b). The condition Eq. (17b) means that the incident linear polarization is reconstructed at the joint plane for both the given polychromatic beam and the spectral component ω_0. For the component ω_0, the values of $\Delta\phi$ being multiples of $\pm 0.5 \times 2\pi$ correspond to linearly polarized states between the segments, while the multiples of $\pm 0.25 \times 2\pi$ provide SoPs of the highest ellipticity possible for given α (circular polarization only for $\alpha = \pi/4 + k\pi/2$, $k = 0, 1, 2, 3$).

In real devices $\Delta\phi$ is mostly related with mechanical strain or temperature fluctuations affecting the birefringence. In this research, however, it is assumed that temperature and all environmental parameters are stable and variations of τ_1' are realized by changing the system parameter L_1. We then define a variable length of the first segment L_1' related with the retardation change $\Delta\phi$:

$$L_1'(\Delta\phi) = L_1^{(0)} + \frac{c}{\Delta n \omega_0}\Delta\phi, \tag{18}$$

where $L_1^{(0)}$ is obtained by the minimal adjustment of the given system parameter L_1 sufficient to satisfy Eq. (17b). It is also assumed that the second segment is scaled proportionally, so that $L_2' = 2L_1'$.

The numerical experimentation has been based on the following relations: (a) $\mathrm{DoP}(\alpha, \theta)$ and (b) $\mathrm{DoP}(\alpha, \Delta\phi)$ for given exemplary parameters of crystal depolarizer and light spectrum where α is the orientation angle of the linear polarization of the incident light and θ is the twist angle between the fast axes of the birefringent segments (Fig. 2). As the azimuth α represents arbitrary variations of SoP of the beam that is to be depolarized, only the extreme values over the full α angle are plotted.

In most cases, however, the global extrema of $\mathrm{DoP}(\alpha, \psi)$ are of the interest, where $\psi \in [-45°, +45°]$ denotes the ellipticity of the SoP of the incident, fully polarized beam. In particular, the global maximum of $\mathrm{DoP}(\alpha, \psi)$ determines uncertainty of the measurement performed by an optical device using the depolarizer. It should be pointed out that extreme values of $\mathrm{DoP}(\alpha, \psi)$ can be easily estimated using plots of $\max_\alpha\{\mathrm{DoP}(\alpha, \Delta\phi)\}$ with $\psi = 0$ assumed, provided that the spectrum of light is not too wide. It is done by use of a property of polarized light that tells that every polarization ellipse can be obtained by a cascade of a rotary polarizer and a variable linear retarder [1]. In our case it means that variance of ψ at input can be simulated by variance of $\Delta\phi$ in the range $[-\pi/2, +\pi/2]$ for the ω_0 component. For the polychromatic beam, it is an approximation because the change of $|\gamma_{11}(\tau_1)|$ related with $\Delta\phi$ variance is neglected as well as the nonperiodical behavior of $\mathrm{Re}\{\gamma_{11}(\tau)\}$.

6. Input Data for Numerical Tests

The three models of depolarization have been tested versus two sets of the light source and the Lyot depolarizer parameters, listed in Table 1. The two test cases have been analyzed as follows.

1. All three DoP computation methods have been applied for the spectrum "SLD" (Fig. 3) of a commercial superluminescent diode SLD-37-MP from Superlum, Ltd. (FWHM ≈ 47 nm) in order to (a) determine whether the proposed model agrees with M–S matrix formalism for polychromatic light, as expected and (b) analyze the error made by the approximate solution by Mochizuki [8] in case of power spectral density distribution not symmetrical with respect to ω_0. Parameters of the Lyot depolarizer are modeled on a commercial device from Edmund Optics designed for wavelength range 200–2300 nm and minimum bandwidth FWHM = 50 nm assuring 85% depolarization.

2. In order to verify whether the differences in predictions observed in point 1 were caused by irregularity of the spectrum of light, the same comparison has been performed for the symmetrical (Gaussian) equivalent of the SLD spectrum ("Gss" in Fig. 3) exhibiting similar shape of the coherence function. Additionally, two nonstandard values of the second segment length have been examined.

The three power spectra $G(\omega)$ used in simulations are depicted in Fig. 3. The corresponding functions $|\gamma_{11}(\tau)|$ have been plotted in accordance with the Wiener–Khintchine theorem Eqs. (5) and (4). The continuous degree of coherence function of the discrete data SLD has been obtained numerically

Table 1. Two Sets of Parameters for Numerical Tests[a]

#	Spectrum	FWHM	$\lambda_0 = 2\pi c/\omega_0$	L_1	L_2	Δn
1.	SLD-37-MP (SLD)	47.2 nm	841 nm	2 mm	4 mm	0.009
2.	Gaussian (Gss)	28.3 nm	841 nm	2 mm	4, 2, 0 mm	0.009

[a]FWHM, full width at half maximum; c, speed of light in vacuum; $L_1 + L_2$, total length of the depolarizer; Δn, birefringence of the crystals.

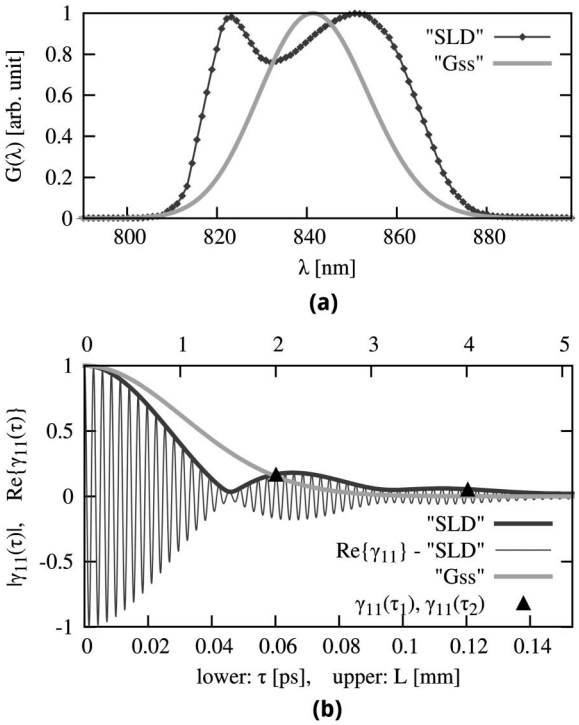

Fig. 3. Characteristics of light spectra for numerical experiments. (a) Spectral density distributions: SLD, commercial superluminescent LED; Gss, a symmetrical equivalent of SLD. (b) Corresponding courses of degree of coherence versus time delay τ induced in a quartz crystal of length L (the upper axis); the two marked points refer to the time delays τ_1 and τ_2 induced by the segments of the commercial 6 mm long quartz depolarizer.

through the inverse Fourier series:

$$\gamma_{11}(\tau) = \frac{\sum_{n=1}^{N} G(\omega_n) e^{-i\omega_n \tau}}{\sum_{n=1}^{N} G(\omega_n)}, \tag{19}$$

where $N = 100$ is the number of power density samples equidistant in the angular frequency domain. The profile $G(\omega_n)$ is obtained from a data set $G(\lambda_n)$ [Fig. 3(a)] through a numerical procedure taking into account the nonlinear relation between the two domains. Thus, the range of frequencies ω_n strictly corresponds to the wavelength range shown in Fig. 3(a).

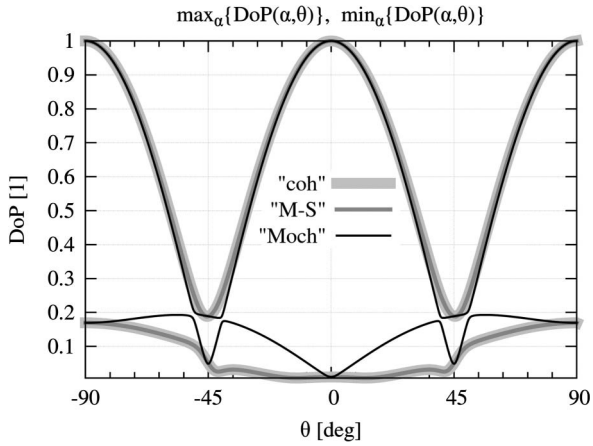

Fig. 4. Comparison for the three models' predictions for SLD spectrum (superluminescent diode). Extreme values of DoP(α) versus the twist angle θ between the segments are plotted. Depolarizer segments thickness ratio is 1:2, linear polarization of the incident beam is reconstructed at the joint plane: $\Delta\phi = 0$.

7. Numerical Results

In this section the three considered computation methods, the M–S formalism, Eq. (12) by Mochizuki [8] and the proposed coherence-based model Eqs. (11) and (2b) will be abbreviated to "M–S," "Moch," and "coh," respectively. The two spectral profiles are called SLD and Gss in accordance with Table 1 and Fig. 3. For the sake of simplicity, the symbol L_1 is used in place of the variable L_1' [Eq. (18)].

A. Data Set 1: Comparison for SLD Light Source

The results are presented in Figs. 4 and 5. The plot in Fig. 4 shows the influence of the twist angle θ between the birefringent segments with thickness ratio 1:2 in the case when the incident linear polarization is reconstructed at the joint plane: $\Delta\phi = 0$. It appears that the proposed method coh agrees with the M–S formalism in full range of θ, unlike the approximate Moch model. In particular, the formula by

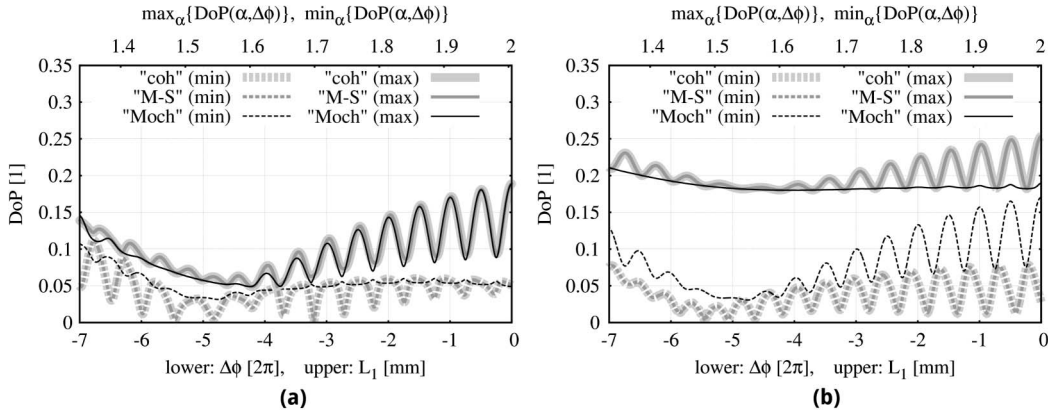

Fig. 5. Comparison for the three models' predictions for SLD spectrum (superluminescent diode). Extreme values of DoP(α) are plotted versus the length of the first crystal L_1 (upper axis) and corresponding change of retardance $\Delta\phi$ (lower axis) for the twist angle between the segments: (a) $\theta = 45°$ and (b) $\theta = 40°$. $L_2 = 2L_1$.

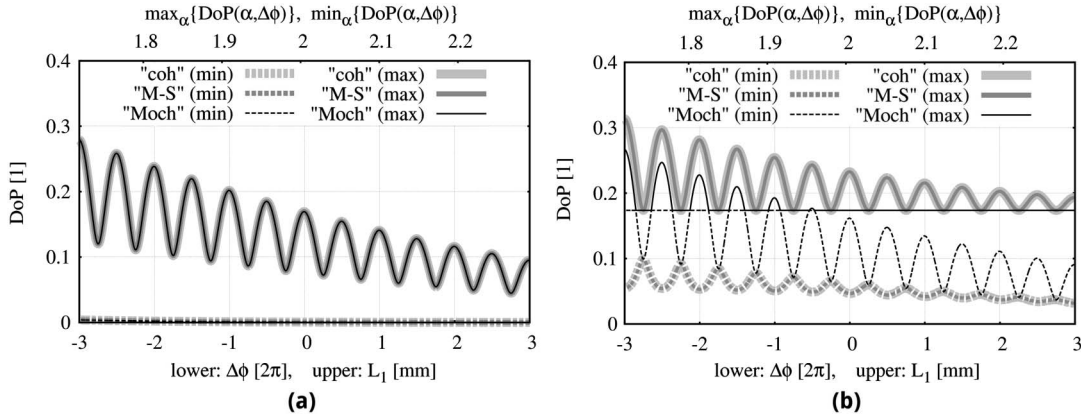

Fig. 6. Comparison for the three models' predictions for Gss spectrum (Gaussian equivalent of SLD). Extreme values of DoP(α) are plotted versus the length of the first crystal L_1 (upper axis) and corresponding change of retardance $\Delta\phi$ (lower axis) for the twist angle between the segments: (a) $\theta = 45°$ and (b) $\theta = 40°$. $L_2 = 2L_1$.

Mochizuki [8] underestimates the global maxima of DoP(α) when θ is close but not equal to 45°.

The values $\theta = 45°$ and $\theta = 40°$ have been chosen for closer study involving the dependency on $\Delta\phi$ in an exemplary range; the results are depicted in Figs. 5(a) and 5(b), respectively. Taking into account that the SLD spectrum is not far from obeying the quasi-monochromatic approximation, the following conclusions can be made here.

For the optimal Lyot configuration ($\theta = 45°$ and $L_2 = 2L_1$) the proposed model coh is in full agreement with the matrix formalism M–S. The approximated model by Mochizuki [8], which is equivalent with the formula from [7] in this case, underestimates the global maximum of DoP(α, ψ) in regions where $|\gamma_{11}(L_1)| \approx |\gamma_{11}(L_2)|$ [see Fig. 3(b)]. In the analyzed example the relative error reaches 15% for DoP ≈ 0.1. For the modified Lyot depolarizer, with $\theta = 40°$, the proposed model coh is still in full agreement with the matrix formalism M–S. The approximated model by Mochizuki [8] underestimates the global maximum of DoP(α, ψ) with relative error up to 25% for DoP ≈ 0.25.

B. Data Set 2: Comparison for a Gaussian Equivalent of SLD Spectrum

The results are presented in Figs. 6 and 7. All the tests confirm the accuracy of the proposed description "coh."

Comparing Figs. 5(a) and 6(a) leads to a conclusion that, in case of the optimal Lyot configuration, the influence of the irregularity of the spectrum shape on the performance of the depolarizer is very little. Thus, the models [7,8] provide a good approximation for residual DoP of light from typical superluminescent diodes even if the requirement of the spectrum symmetry is strongly violated. Some errors occur only in regions where $|\gamma_{11}(L_1)| \approx |\gamma_{11}(L_2)|$, i.e., where both segments introduce equal decorrelation between components parallel to their birefringence axes [compare Fig. 5(a) with Fig. 3(b)].

Conclusions arising from Figs. 5(b) and 6(b) are different. It appears that, for a slightly disturbed twist angle θ, the inconsistency between Moch and the two other models cannot be explained by irregularity of the SLD spectrum. As the spectral power distribution meets the requirements related with Eq. (12), the model [8] apparently exhibits an unexpected defect here. The related error, however, is significant only for L_1 values comparable with the coherence length of light.

The plots in Fig. 7 illustrate another unexpected property of the Moch formula in the case of a spectral profile that satisfies conditions restricting the solution [8]. It appears that one can obtain nonphysical DoP > 1 values when DoP ≈ 1 is expected, that is, when the beam starts to propagate in L_1 or in case of almost full compensation of depolarization, $L_2 \approx$

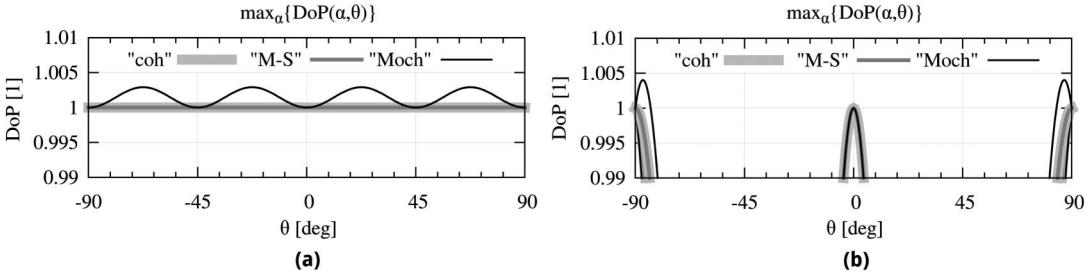

Fig. 7. Comparison for the three models' predictions for Gss spectrum (Gaussian equivalent of SLD). Global maximum of DoP(α) is plotted versus the twist angle θ between the segments of the depolarizer. The segments' lengths are (a) $L_1 = 2$ mm, $L_2 = 0$ and (b) $L_1 = L_2 = 2$ mm. Linear polarization of the incident beam is reconstructed at the joint plane $\Delta\phi = 0$.

$L_1 >> 0$ with $\theta \approx \pm 90°$. These two situations are illustrated in Figs. 7(a) and 7(b), respectively, using parameters of the commercial Lyot depolarizer with modified length of the second quartz crystal. The effect in Fig. 7(a) is limited by thickness of the first crystal; for $L_1 = 0.047$ mm, we obtain DoP ≈ 1.2.

The nonphysical behavior of the Moch formula Eq. (12) arises from persistence of terms dependent on θ after $\tau_2 = 0$ is substituted. It can be also shown that the term $\cos(\omega_0 \tau)$, describing SoP at the joint plane, does not vanish as well, causing additional false rapid DoP oscillations along the propagation axis (not plotted here). The proposed coherence-based Eqs. (11) and (2b) do not cause any of these problems.

8. Conclusions

A novel analytical formula describing performance of a family of static depolarizers consisting of two segments of anisotropic medium, including the Lyot depolarizer configuration, has been presented. Unlike the previous models [7,8], which are limited to symmetrical spectra, the proposed solution is valid for light of any spectral power distribution shape. The full derivation of the expressions, based on the theory of optical coherence [9–11], is provided along with geometrical interpretation of all the terms and with a numerical comparison with the previous models. The numerical tests have been performed using real-world exemplary parameters for both the depolarizer and the illuminating light. They proved that the proposed coherence-based description is fully consistent with the M–S matrix formalism for broadband light [5,6], which suggests that these approaches are algebraically equivalent.

Following this consistency, the range of accuracy of the classical coherence-based solutions [7,8] has been verified. The results show that, in the case of the optimal configuration of the Lyot depolarizer, these models offer a good approximation when applied to an irregular spectrum of light from a superluminescent diode. For other configurations, however, it has been pointed out that the solution by Mochizuki [8] can give inaccurate or nonphysical predictions despite the symmetricity of the spectral profile of the passing light. The model proposed in this paper is free of those defects.

References

1. D. H. Goldstein and E. Collett, *Polarized Light* (Dekker, 2003).
2. P. Shen and J. C. Palais, "Passive single-mode fiber depolarizer," Appl. Opt. **38**, 1686–1691 (1999).
3. M. Martinelli and J. Palais, "Dual fiber-ring depolarizer," J. Lightwave Technol. **19**, 899–905 (2001).
4. B. Lyot, "Recherche sur la polarisationde la lumière des planètes et de quelques substances terrestres," in *Annales de l'Observatoire de Paris (Meudon)*, **Tome VIII, Facs. I** (1929).
5. B. H. Billings, "A monochromatic depolarizer," J. Opt. Soc. Am. **41**, 966–968 (1951).
6. A. P. Loeber, "Depolarization of white light by a birefringent crystal. II. The Lyot depolarizer," J. Opt. Soc. Am. **72**, 650–656 (1982).
7. W. K. Burns, "Degree of polarization in the Lyot depolarizer," J. Lightwave Technol. **1**, 475–479 (1983).
8. K. Mochizuki, "Degree of polarization in jointed fibers: the Lyot depolarizer," Appl. Opt. **23**, 3284–3288 (1984).
9. L. Mandel and E. Wolf, *Optical Coherence and Quantum Optics* (Cambridge University, 1995).
10. E. Wolf, "Unified theory of coherence and polarization of random electromagnetic beams," Phys. Lett. A **312**, 263–267 (2003).
11. E. Wolf, *Introduction to the Theory of Coherence and Polarization of Light* (Cambridge University, 2007).
12. K. Oka and T. Kato, "Spectroscopic polarimetry with a channeled spectrum," Opt. Lett. **24**, 1475–1477 (1999).
13. E. I. Alekseev and E. N. Bazarov, "Theoretical basis of the method for reducing drift of the zero level of the output signal of a fiber-optic gyroscope with the aid of a Lyot depolarizer," Sov. J. Quantum Electron. **22**, 834–839 (1992).
14. P. L. Makowski and A. W. Domański, "Degree of polarization fading of light passing through birefringent medium with optical axis variation," Proc. SPIE **7745**, 77450J (2010).
15. J. Sakai, S. Machida, and T. Kimura, "Existence of eigen polarization modes in anisotropic single-mode optical fibers," Opt. Lett. **6**, 496–498 (1981).